

Search for $\delta^{\pm\pm}$ with new decay patterns at the LHC

Chuan-Hung Chen^{a*} and Takaaki Nomura^{a†}

^a*Department of Physics, National Cheng-Kung University, Tainan 701, Taiwan*

(Dated: March 3, 2015)

Abstract

A study of searching for doubly charged Higgs ($\delta^{\pm\pm}$) is performed in two-Higgs-doublet extension of the conventional type-II seesaw model. We find that a fantastic mixing effect between singly charged Higgs of Higgs doublet and of triplet is arisen from the scalar potential. The mixing leads to following intriguing phenomena: (a) the mass splittings in triplet particles are magnified, (b) QCD processes dominate the production of $\delta^{\pm\pm}$, and (c) new predominant decay channels of $\delta^{\pm\pm}$ are $\delta^{\pm\pm} \rightarrow W^{\pm[*]} H_{1(2)}^{\pm(*)}$, but not $\delta^{\pm\pm} \rightarrow (\ell^{\pm}\ell^{\pm}, W^{\pm}W^{\pm})$ which are usually discussed in the literature. With luminosity of 40 fb^{-1} and collision energy of 13 TeV, we demonstrate that $\delta^{\pm\pm}$ with mass below 330 GeV could be observed at the 5σ level. Moreover, when the luminosity approaches to 300 fb^{-1} , the observed mass of $\delta^{\pm\pm}$ could reach up to 450 GeV.

* Email: physchen@mail.ncku.edu.tw

† Email: nomura@mail.ncku.edu.tw

I. INTRODUCTION

The origin of the masses of standard model (SM) particles from spontaneous electroweak symmetry breaking, called Higgs mechanism, is supported by the new observed scalar boson with a mass around 125 GeV, measured by ATLAS [1] and CMS [2]. Following the same concept, the mystery of tiny neutrino masses may be solved in the framework of multiple Higgs fields without introducing the heavy singlet right-handed neutrinos [3], in which the representative model is the Higgs triplet extension of the SM [4] and here we call it as the conventional type-II seesaw model (CTTSM).

The novel feature of a Higgs triplet model is the existence of a doubly charged Higgs, hereafter denoted by $\delta^{\pm\pm}$. Therefore, in order to detect the Higgs triplet particles, the searches for $\delta^{\pm\pm}$ at colliders have been studied widely by theorists [6–19] and experimentalists [20–23]. The collider signatures ordinarily depend on the vacuum expectation value (VEV) of the neutral triplet field, v_Δ , which is the source of neutrino masses. For instance, if $v_\Delta \ll 10^{-4}$ GeV or the associated leptonic Yukawa couplings are relatively large, it is found that the doubly charged Higgs mainly decays into a pair of same-sign charged leptons, i.e. $\delta^{\pm\pm} \rightarrow \ell^\pm \ell^\pm$ ($\ell = e, \mu$) [6, 17]. However, if $v_\Delta \gg 10^{-4}$ GeV or the associated leptonic Yukawa couplings are relatively small, the dominant decay channel of $\delta^{\pm\pm}$ is $\delta^{\pm\pm} \rightarrow W^\pm W^\pm$ [6, 17]. Therefore, the searches for $\delta^{\pm\pm}$ at colliders usually are focused on the decay channels of same-sign leptons or same-sign W bosons. Consequently, if one assumes that $\delta^{\pm\pm}$ is 100% decaying into leptons, the experimental lower bound of its mass now is around 400 GeV [21, 22]. If WW channel is dominant, the mass limit of $\delta^{\pm\pm}$ now is up to 300 (550) GeV when $v_\Delta = 25(35)$ GeV [23].

Historically, the two-Higgs-doublet model (THDM) was proposed for solving the weak and strong CP problems [24, 25]. In spite of the original motivation, THDM itself provides rich phenomena in particle physics. By the new discovery of 125 GeV scalar boson at ATLAS and CMS, the phenomenology of THDM has been further investigated broadly in the literature, e.g. Refs. [26–28]. By combining the issue of neutrino physics, it is intriguing to explore the fantastic effects in the model involving two Higgs doublets (THDs) and one Higgs triplet. Indeed, we find that the production and decay patterns of doubly charged Higgs will be completely changed when the second Higgs doublet is added to the CTTSM.

In the THD type-II seesaw model, although we have new interacting terms from various

sectors, the most attractive new effects are the dimension-3 terms in scalar potential, read by $\mu_j H_j^T i\tau_2 \Delta^\dagger H_k$ ($j, k = 1, 2$), where H and Δ are the Higgs doublet and triplet, respectively. Since the coefficients μ_j are of order of electroweak (EW) scale, the new terms lead a large mixing angle between the singly charged Higgs of doublet (H^\pm) and of triplet (δ^\pm). According to our previous study [29], if we assume the Higgs triplet particles are heavier than the Higgs doublets, due to the new mixing effect, we have the interesting phenomena: (I) the charged Higgs H^\pm could be lighter than that in type-II THDM, (II) even we set the degeneracy of $m_{\delta^{\pm\pm}} = m_{\delta^\pm}$, the mass splitting between $\delta^{\pm\pm}$ and δ^\pm could be magnified, (III) the branching fractions for $\delta^{\pm\pm} \rightarrow W^\pm H_i^\pm$ are much larger than those for $\delta^{\pm\pm} \rightarrow (\ell^\pm \ell^\pm, W^\pm W^\pm)$. Due to these new characters, one expects that the signals of $\delta^{\pm\pm}$ in the THD type-II seesaw model are different from those signals in other triplet models.

For exploring the signals of $\delta^{\pm\pm}$, in this paper we study its various production processes. Since now the Higgs doublets could couple to the Higgs triplet, unlike the cases in CTTSM and Georgi-Machacek model [10, 30] where EW processes dominate, we find that the doubly charged Higgs in our model is predominantly produced by QCD processes, indicated by $pp \rightarrow H_2^+ \bar{t} b (H_2^- t \bar{b}) \rightarrow \delta^{++} W^- \bar{t} b (\delta^{--} W^+ t \bar{b})$ and $\bar{b}(b)g \rightarrow H_2^+ \bar{t} (H_2^- t) \rightarrow \delta^{++} W^- \bar{t} (\delta^{--} W^+ t)$. Due to more jets involved in the production and decays of $\delta^{\pm\pm}$, the selected events for simulation are $\ell^\pm \ell^\pm + n\text{jets}$ with $n \geq 4$. For reducing the possible background events, we propose several kinematical cuts on the second highest transverse-momentum lepton and the invariant mass of the same-sign dilepton. Additionally, we also study the discovery potential for 5σ significance with the collision energy of 13 TeV and the designed luminosity at the LHC.

We organize the paper as follows. In Sec. II, we briefly discuss the relevant new interactions originated in Yukawa sector, gauge invariant kinetic terms of involved scalar fields and the scalar potential. The new characters of doubly charged Higgs is also introduced. We investigate the production and decays of doubly charged Higgs and the branching fractions of singly charged Higgses in Sec. III. The detailed simulation on signals and backgrounds are given in Sec. IV. We summarize the findings in Sec. V.

II. NEW CHARACTERS OF DOUBLY CHARGED HIGGS

For studying the detection of doubly charged Higgs in the THD and one Higgs triplet model, we first summarize the relevant interactions with $\delta^{\pm\pm}$. The detailed introduction to the model could refer to Ref. [29]. For satisfying the gauge symmetry of the SM, $\delta^{\pm\pm}$ can only directly couple to leptons in leptonic Yukawa sector and the couplings are expressed by

$$\begin{aligned}\mathcal{L}_{\delta^{\pm\pm}\ell\ell} &= \frac{1}{2}\ell'^T C \mathbf{h} P_L \ell' \delta^{++} + h.c., \\ \mathbf{h} &= \frac{\sqrt{2}}{v_\Delta} U_{\text{PMNS}}^* \mathbf{m}_\nu^{\text{dia}} U_{\text{PMNS}}^\dagger,\end{aligned}\tag{1}$$

where ℓ' denotes the charged leptons, $\mathbf{m}_\nu^{\text{dia}}$ is the diagonalized neutrino mass matrix and U_{PMNS} is the Pontecorvo-Maki-Nakagawa-Sakata (PMNS) matrix [31, 32]. From Eq. (1), one can see that the typical coupling of $\delta^{\pm\pm}$ to lepton-pair is proportional to m_ν/v_Δ . If we assume that the masses of neutrinos are measured well in experiments, the partial decay rates for $\delta^{\pm\pm} \rightarrow \ell'^\pm \ell'^\pm$ depend on the value of $1/v_\Delta$. By the gauge invariant kinetic terms of Higgs triplet, the couplings of $\delta^{\pm\pm}$ to gauge bosons are written as

$$\begin{aligned}\mathcal{L}_{\delta^{\pm\pm}GG} &= -i \frac{g}{\cos \theta_W} (1 - 2 \sin^2 \theta_W) \delta^{--} (\partial_\mu \delta^{++}) Z^\mu - i 2e \delta^{--} (\partial_\mu \delta^{++}) A^\mu \\ &\quad - i g (\partial_\mu \delta^{++}) \delta^- W^{-\mu} + i g \delta^{++} (\partial_\mu \delta^-) W^{-\mu} + \frac{g^2 v_\Delta}{\sqrt{2}} \delta^{++} W_\mu^- W^{-\mu} + h.c.,\end{aligned}\tag{2}$$

where δ^\pm are the singly charged Higgs of Higgs triplet. Clearly, the branching fraction for $\delta^{\pm\pm} \rightarrow W^\pm W^\pm$ depends on the magnitude of v_Δ . According to Eq. (1) and Eq. (2), one can realize that in CTSM, the main decays of $\delta^{\pm\pm}$ are through the two-body decays $\delta^{\pm\pm} \rightarrow (\ell^\pm \ell^\pm, W^\pm W^\pm)$ and three-body decays $\delta^{\pm\pm} \rightarrow W^{\pm(*)} \delta^{\pm(*)}$, in which the off-shell condition relies on the mass of δ^\pm .

Since there is only one $\delta^{++(-)}$ in the model, the property changes of $\delta^{\pm\pm}$ are arisen from the new interacting terms in scalar potential. In order to clearly understand the effects, we

write the gauge invariant scalar potential as

$$\begin{aligned}
V(H_1, H_2, \Delta) &= V_{H_1 H_2} + V_\Delta + V_{H_1 H_2 \Delta}, \\
V_{H_1 H_2} &= m_1^2 H_1^\dagger H_1 + m_2^2 H_2^\dagger H_2 - m_{12}^2 (H_1^\dagger H_2 + h.c.) + \lambda_1 (H_1^\dagger H_1)^2 \\
&\quad + \lambda_2 (H_2^\dagger H_2)^2 + \lambda_3 H_1^\dagger H_1 H_2^\dagger H_2 + \lambda_4 H_1^\dagger H_2 H_2^\dagger H_1 + \frac{\lambda_5}{2} \left[(H_1^\dagger H_2)^2 + h.c. \right], \\
V_\Delta &= m_\Delta^2 \text{Tr} \Delta^\dagger \Delta + \lambda_9 (\text{Tr} \Delta^\dagger \Delta)^2 + \lambda_{10} \text{Tr} (\Delta^\dagger \Delta)^2, \\
V_{H_1 H_2 \Delta} &= (\mu_1 H_1^T i \tau_2 \Delta^\dagger H_1 + \mu_2 H_2^T i \tau_2 \Delta^\dagger H_2 + \mu_3 H_1^T i \tau_2 \Delta^\dagger H_2 + h.c.) \\
&\quad + \left(\lambda_6 H_1^\dagger H_1 + \bar{\lambda}_6 H_2^\dagger H_2 \right) \text{Tr} \Delta^\dagger \Delta + H_1^\dagger (\lambda_7 \Delta \Delta^\dagger + \lambda_8 \Delta^\dagger \Delta) H_1 \\
&\quad + H_2^\dagger (\bar{\lambda}_7 \Delta \Delta^\dagger + \bar{\lambda}_8 \Delta^\dagger \Delta) H_2,
\end{aligned} \tag{3}$$

where $V_{H_1 H_2}$ and V_Δ stand for the scalar potential of THD and of pure triplet, and $V_{H_1 H_2 \Delta}$ is the part involving H_1 , H_2 and Δ . By taking the VEVs of $H_{1,2}$ and Δ to be $v_{1,2}$ and v_Δ respectively, the vacuum stability requires

$$v_\Delta \approx \frac{1}{\sqrt{2}} \frac{\mu_1 v_1^2 + \mu_2 v_2^2 + \mu_3 v_1 v_2}{m_\Delta^2 + (\lambda_6 + \lambda_7) v_1^2 / 2 + (\bar{\lambda}_6 + \bar{\lambda}_7) v_2^2 / 2}. \tag{4}$$

Due to the precision measurement of ρ -parameter, we have $v_\Delta \ll v = \sqrt{v_1^2 + v_2^2}$ and just keep the leading power for v_Δ in Eq. (4). By this result, we see that when $\mu_2 = \mu_3 = 0$, the small v_Δ indicates the small μ_1 or large m_Δ in CTSM. However, when the μ_2 and μ_3 effects are introduced, the necessity of small v_Δ could be accommodated by the massive parameters $\mu_{1,2,3}$ and m_Δ , where they could be in the same order of magnitude. Hence, the small value of v_Δ could be adjusted by the free parameters of the new scalar potential, without introducing a hierarchy to the massive parameters.

It is known that in CTSM, the mixing effect of Higgs doublet and triplet is related to the suppressed factor v_Δ/v . However, an interesting mixing effect could be induced in the THD extended type-II seesaw model when $\mu_{1,2,3}$ in Eq. (3) are all as large as EW scale. For displaying the influence of $\mu_{1,2,3}$, we take the singly charged Higgses as the illustrator. The similar discussions are also suitable for neutral scalars [29]. As known, one physical charged Higgs H^\pm exists in the conventional THD model and a massive Higgs triplet provides a singly charged Higgs δ^\pm . If we take the approximation of $v_\Delta/v \approx 0$, we find that the mixture of δ^\pm with charged Goldstone boson of THD could be ignored. For simplifying the analysis and preserving the requirement of $v_\Delta \ll v$, in the numerical estimates, we adopt the relation

$$\mu_3 \sim -\frac{\mu_1 v_1^2 + \mu_2 v_2^2}{v_1 v_2}.$$

By Eq. (3) and decoupling from the Goldstone boson, the mass matrix of singly charged Higgses in our model could be formulated by a 2×2 matrix and expressed by

$$(H^- \delta^-) \begin{pmatrix} m_{H^- H^+}^2 & m_{H^- \delta^+}^2 \\ m_{H^- \delta^+}^2 & m_{\delta^- \delta^+}^2 \end{pmatrix} \begin{pmatrix} H^+ \\ \delta^+ \end{pmatrix}, \quad (5)$$

where the elements of mass matrix are found by

$$\begin{aligned} m_{H^- H^+}^2 &\equiv m_{H^\pm}^2 = \frac{m_\pm^2}{\sin \beta \cos \beta}, \quad m_\pm^2 = m_{12}^2 - \frac{\lambda_4 + \lambda_5}{2} v_1 v_2, \\ m_{H^- \delta^+}^2 &= \frac{v}{2 \sin \beta \cos \beta} [\mu_1 \cos^4 \beta - \mu_2 \sin^4 \beta + (\mu_1 - \mu_2) \sin^2 \beta \cos^2 \beta], \\ m_{\delta^- \delta^+}^2 &\equiv m_{\delta^\pm}^2 = m_\Delta^2 + \frac{v_1^2}{4} (2\lambda_6 + \lambda_7 + \lambda_8) + \frac{v_2^2}{4} (2\bar{\lambda}_6 + \bar{\lambda}_7 + \bar{\lambda}_8). \end{aligned} \quad (6)$$

We see that the off-diagonal element is associated with the parameters $\mu_{1,2}$ and $\tan \beta = v_2/v_1$. The physical charged Higgs states could be regarded as the combination of H^\pm and δ^\pm and their mixture could be parametrized by

$$\begin{pmatrix} H_1^\pm \\ H_2^\pm \end{pmatrix} = \begin{pmatrix} \cos \theta_\pm & \sin \theta_\pm \\ -\sin \theta_\pm & \cos \theta_\pm \end{pmatrix} \begin{pmatrix} H^\pm \\ \delta^\pm \end{pmatrix}. \quad (7)$$

The masses of charged Higgs particles and their mixing angle are derived as

$$\begin{aligned} (m_{H_{1,2}^\pm})^2 &= \frac{1}{2} (m_{\delta^\pm}^2 + m_{H^\pm}^2) \mp \frac{1}{2} [(m_{\delta^\pm}^2 - m_{H^\pm}^2)^2 + 4m_{H^- \delta^+}^4]^{1/2}, \\ \tan 2\theta_\pm &= -\frac{2m_{H^- \delta^+}^2}{m_{\delta^\pm}^2 - m_{H^\pm}^2}. \end{aligned} \quad (8)$$

Here H_1^\pm is identified as the lighter charged Higgs. Clearly, the magnitude of mixing angle θ_\pm relies on the massive parameters $\mu_{1,2}$. In this paper, we are going to explore the influence of large mixing angle θ_\pm on the search for the doubly charged Higgs. With the new mixing effect, we present the couplings of $\delta^{\pm\pm}$ to the physical states H_i^\pm and W^\pm in Table I. By the Table, we see that the involved free parameter for the vertex $\delta^{\pm\pm}-H_i^\mp-W^\mp$ is only the angle θ_\pm . Although the coupling for the vertex $\delta^{\pm\pm}-H_i^\mp-H_i^\mp$ could be comparable with that for $\delta^{\pm\pm}-H_i^\mp-W^\mp$, due to phase space suppression, the decay rate for $H_i^\pm H_i^\pm$ mode usually will be smaller than that for $H_i^\pm W^\pm$ mode, except the case of $\tan \beta = 1$ with $\mu_1 = \mu_2$ and the case constrained by kinematic requirement [29].

Although δ^\pm cannot couple to quarks directly, however due to the new mixing effect in Eq. (7), the two physical charged Higgses now can interact with quarks and the interactions

Vertex	Coupling	Vertex	Coupling
$\delta^{\pm\pm} H_2^\mp W_\mu^\mp$	$-ig \cos \theta_\pm (p_{\delta^{\pm\pm}} - p_{H_2^\mp})_\mu$	$\delta^{\pm\pm} H_1^\mp W_\mu^\mp$	$-ig \sin \theta_\pm (p_{\delta^{\pm\pm}} - p_{H_1^\mp})_\mu$
$\delta^{\pm\pm} H_{1(2)}^\mp H_{1(2)}^\mp$	$2(\mu_1 + \mu_2) \cos^2 \theta_\pm (\sin^2 \theta_\pm)$	$\delta^{\pm\pm} H_1^\mp H_2^\mp$	$2(\mu_1 + \mu_2) \cos \theta_+ \sin \theta_+$

TABLE I: The couplings of $\delta^{\pm\pm}$ to $H_{1,2}^\pm$ and W^\pm .

with fermions are formulated by

$$\begin{aligned}
\mathcal{L}_{H_i^\pm f f'} &= \frac{\sqrt{2}}{v} \left[\bar{u} \left(\tan \beta V_{CKM} \mathbf{m}_D P_R + \cot \beta \mathbf{m}_U V_{CKM}^\dagger P_L \right) d + \tan \beta \bar{\nu} \mathbf{m}_\ell P_R \ell' \right] \\
&\times (\cos \theta_\pm H_1^+ - \sin \theta_\pm H_2^+) + h.c. ,
\end{aligned} \tag{9}$$

where we suppress all flavor indices, $u^T = (u, c, t)$ and $d^T = (d, s, b)$ denote the up and down type quarks, $\nu^T = (\nu_e, \nu_\mu, \nu_\tau)$ and $\ell^T = (e, \mu, \tau)$ are the neutrinos and charged leptons, V_{CKM} is the Cabibbo-Kobayashi-Maskawa (CKM) matrix, $\mathbf{m}_{D(U)}$ is the diagonalized mass matrix of down (up) type quarks, and $P_{R,L} = (1 \pm \gamma_5)/2$. Note that the Yukawa couplings of δ^+ and leptons are assumed to be small and negligible, thus we do not show them in Eq. (9).

III. PRODUCTION AND DECAYS OF DOUBLY CHARGED HIGGS

In order to search for the signals of doubly charged Higgs, we need to understand its producing mechanisms and the main decay modes. In the following discussions, we focus on the production of $\delta^{\pm\pm}$ and its decays.

A. Production of doubly charged Higgs at LHC

According to the interactions in Eq. (2) and Table I, we see that the $\delta^{\pm\pm}$ could be produced by EW interactions via s-channel, read as

$$pp \rightarrow Z/\gamma \rightarrow \delta^{++} \delta^{--} , \tag{10}$$

$$pp \rightarrow W^\pm \rightarrow \delta^{\pm\pm} H_{1,2}^\mp . \tag{11}$$

Except the new mixing effect θ_\pm , the production channels are similar to those in CTSM. We note that due to $v_\Delta \ll v$ in our model, the WW fusion is small and negligible. Moreover, with the new effects arisen from μ_i terms in scalar potential, the on-shell $\delta^{\pm\pm}$ could be

produced through the QCD interactions and the relevant processes are given by

$$pp \rightarrow H_2^+ \bar{t} b (H_2^- t \bar{b}) \rightarrow \delta^{++} W^- \bar{t} b (\delta^{--} W^+ t \bar{b}), \quad (12)$$

$$pp \rightarrow H_2^+ \bar{t} (H_2^- t) \rightarrow \delta^{++} W^- \bar{t} (\delta^{--} W^+ t). \quad (13)$$

Since the adopted mass relation is $m_{H_1^\pm} < m_{\delta^{\pm\pm}} < m_{H_2^\pm}$, the on-shell doubly charged Higgs in Eq. (12) and (13) is generated by the decay $H_2^\pm \rightarrow \delta^{\pm\pm} W^\mp$, and then follows the decay $\delta^{\pm\pm} \rightarrow H_1^\pm W^\pm$. The production of $\delta^{\pm\pm}$ through lighter charged Higgs H_1^\pm is off-shell effects and small, we therefore ignore its contributions. For the processes in Eq. (13), the main QCD reaction is associated with the interactions of b-quark and gluons, e.g. $\bar{b}(b)g \rightarrow H_2^+ \bar{t} (H_2^- t)$.

Besides the mass parameters of $H_{1,2}^\pm$ and $\delta^{\pm\pm}$, the involved new free parameters for $\delta^{\pm\pm}$ production are $\sin \theta_\pm$ and $\tan \beta$. It is known that δ^\pm and $\delta^{\pm\pm}$ belong to the same triplet state, after electroweak symmetry breaking, as expected that their mass splitting should be of order of EW scale. For reducing the number of free parameters and guaranteeing to have a positive definite $m_{H_{1,2}^\pm}$ shown in Eq. (8), instead of scanning over the parameter spaces, we set the correlations of parameters for numerical analysis to be

$$\begin{aligned} m_{\delta^\pm} &= m_{\delta^{\pm\pm}} + 100 \text{ GeV}, \\ m_{H^\pm} &= \frac{4}{5} m_{\delta^\pm}, \\ \mu_1 &= -\mu_2 = m_{\delta^\pm} \sin \beta \cos \beta, \end{aligned} \quad (14)$$

where the setting of $\mu_1 = -\mu_2$ leads the couplings of $\delta^{\pm\pm} H_i^\mp H_j^\mp$ in Table I to vanish. Accordingly, the masses of charged Higgs and their mixing angle are obtained by

$$\begin{aligned} (m_{H_{1,2}^\pm})^2 &= m_{\delta^\pm}^2 \left(\frac{41}{50} \mp \frac{1}{2} \left[\frac{81}{625} + \frac{v^2}{m_{\delta^\pm}^2} \right]^{\frac{1}{2}} \right), \\ \tan 2\theta_\pm &= -\frac{25v}{9m_{\delta^\pm}}. \end{aligned} \quad (15)$$

By the simplified formulae, one can see that the new free parameters are reduced to be m_{δ^\pm} and $\tan \beta$. With the parameter settings of Eq. (14), we find that not only the mass relation $m_{H_1^\pm} < m_{\delta^{\pm\pm}} < m_{H_2^\pm}$ can be satisfied, but also the mixing angle θ_\pm in Eq. (15) can be large if m_{δ^\pm} is of $O(100)$ GeV.

For calculating the production cross section of $\delta^{\pm\pm}$, we employ the `CalcHEP 3.6.15` code [33] by implementing the parameters and vertices of our model. With the settings

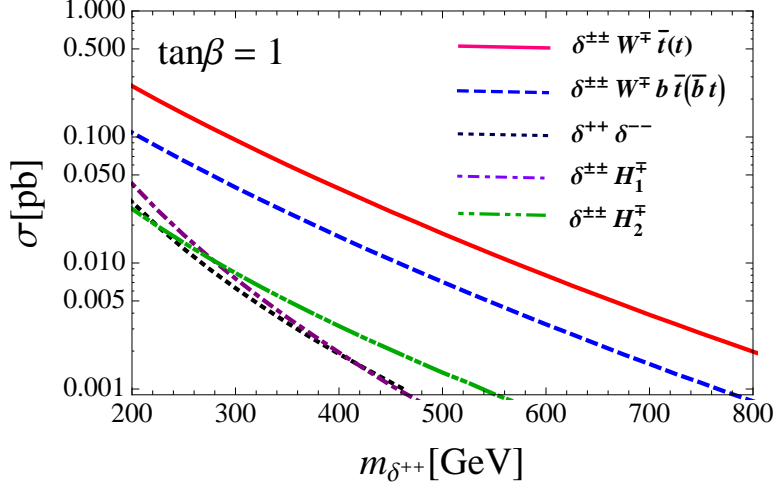


FIG. 1: Production cross sections of the doubly charged Higgs as a function of $m_{\delta^{\pm\pm}}$ for collision energy of 13 TeV at the LHC, where the dotted, dash-dotted and dash-dot-dotted lines denote the EW processes while the solid and dashed lines stand for QCD processes. The settings in Eq. (14) and $\tan\beta = 1$ are adopted.

of Eq. (14), $\tan\beta = 1$ and the results of Eq. (15), we present the production cross sections for the processes in Eqs. (10)-(13) as a function of $m_{\delta^{\pm\pm}}$ in Fig. 1, where the collision energy at LHC is 13 TeV and CTEQ6L PDF [34] is applied, the dotted, dash-dotted and dash-dot-dotted lines denote the EW processes while the solid and dashed lines stand for QCD processes, respectively. Since the contributions of gluons are dominant at pp collision, as expected, the results of QCD production processes are much larger than those of EW ones. For further displaying the influence of $\tan\beta$, we fix $m_{\delta^{\pm\pm}} = 200$ GeV and plot the production cross sections of $\delta^{\pm\pm}$ for QCD processes as a function of $\tan\beta$ in Fig. 2. By the results, we find that the cross section has a minimum and occurs at around $\tan\beta = 7$. The larger production cross sections occur at $\tan\beta \sim O(1)$ or $\sim O(m_t/m_b)$. Based on this result, we concentrate on $\tan\beta = 1$ in our numerical calculations.

B. Branching fractions of $\delta^{\pm\pm}$ and charged Higgs

When the information for $\delta^{\pm\pm}$ production is obtained, we then discuss how the doubly charged Higgs decays. According to the introduced interactions, we know that $\delta^{\pm\pm}$ could decay into $\ell^\pm\ell^\pm$, $W^\pm W^\pm$, $H_i^\pm H_j^\pm$, $W^\pm H_j^\pm$, etc. For fitting the tiny masses of neutrinos, if we

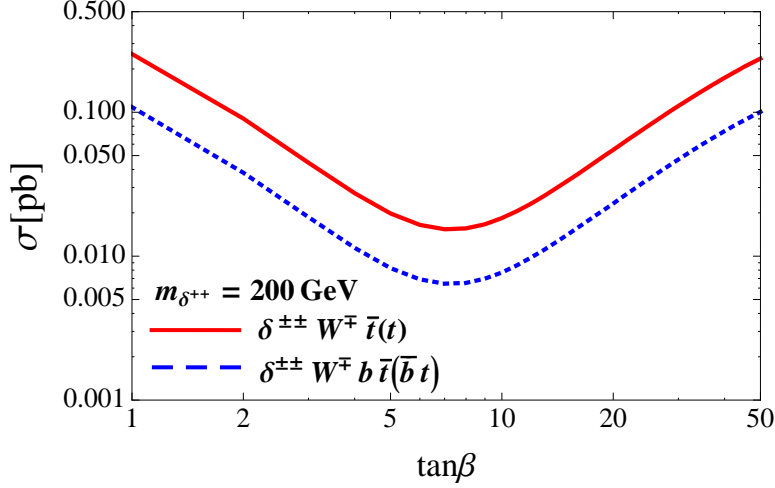


FIG. 2: Production cross sections of $\delta^{\pm\pm}$ as a function of $\tan\beta$ for collision energy of 13 TeV at the LHC, where the solid and dashed lines are the QCD processes in Eq. (12) and (13), respectively. The settings of Eq. (14) and $m_{\delta^{\pm\pm}} = 200$ GeV are used.

adopt the Yukawa couplings of leptons and triplet, $Y_{\ell\ell'}$, and v_Δ to be small simultaneously, then the first two channels could be ignored. Unlike other Higgs triplet models which only focus on either large $Y_{\ell\ell'}$ or large v_Δ , the suppression of lepton-pair and W -pair decays is the new character of our model. With $\mu_1 = -\mu_2$ scheme, the third channel vanishes. Hence, $\delta^{\pm\pm}$ mainly decays into $W^{\pm(*)} H_i^{\pm(*)}$, where W^\pm and H_i^\pm could be on-shell and off-shell, depending on the mass of $\delta^{\pm\pm}$. With the parameter settings of Eq. (14), we present the branching ratios (BRs) for $\delta^{++} \rightarrow W^{+(*)} H_{1,2}^{+(*)}$ in Fig. 3, where the solid line denotes the BRs for the three (four) body decays of $\delta^{++} \rightarrow W^{+(*)} H_{1,2}^{+*}$ and the dashed line is the BR for the three-body decay of $\delta^{++} \rightarrow W^{+*} H_1^+$. Due to our parameter settings, the decays for both on-shell W^\pm and H_1^\pm are suppressed. By the figure, we see that when $m_{\delta^{++}} \gtrsim 300$ GeV, the decays with on-shell W -boson become dominant.

Now we realize that the doubly charged Higgs dominantly decays into one charged Higgs and one W gauge boson in our model. For simulating the $\delta^{\pm\pm}$ events, we further discuss the decays of W and $H_{1,2}^\pm$. Since the decays of W boson are clear in the SM, we just focus on the $H_{1,2}^\pm$ decays. According to Eq. (9), we see that $H_{1,2}^\pm$ could decay to leptons and quarks, in which the couplings to fermions are proportional to the masses of fermions. By neglecting the small mass effects and CKM suppressions, we present the BRs for H_1^+ decays as a function

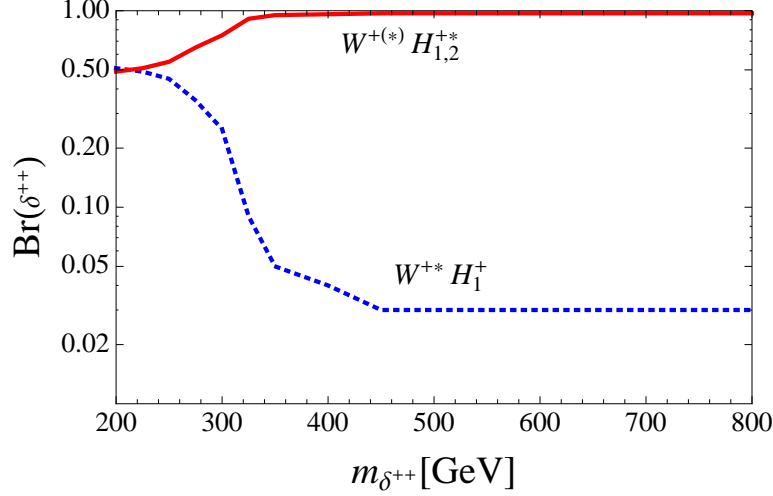


FIG. 3: Branching ratios of doubly charged Higgs decays as a function of $m_{\delta^{\pm\pm}}$.

of $m_{H_1^\pm}$ in Fig. 4 with $\tan\beta = 1$ (left panel) and $\tan\beta = 30$ (right panel). For heavier charged Higgs H_2^\pm , besides the decay channels appearing in H_1^\pm , the decay $H_2^\pm \rightarrow \delta^{\pm\pm} W^\mp$ can also occur with our parameter settings. Hence, the BRs for $\tan\beta = 1$ (left panel) and $\tan\beta = 30$ (right panel) as a function of $m_{H_2^\pm}$ are given in Fig. 5. By the plot, we see clearly that $H_2^+ \rightarrow (\delta^{++} W^-, t\bar{b})$ are the main decay modes and the BR of former is larger than that of latter. Nevertheless, it is worthy to mention that the off-shell H_2^\pm generated in $\delta^{\pm\pm}$ decays will convert into $t\bar{b}(t\bar{b})$.

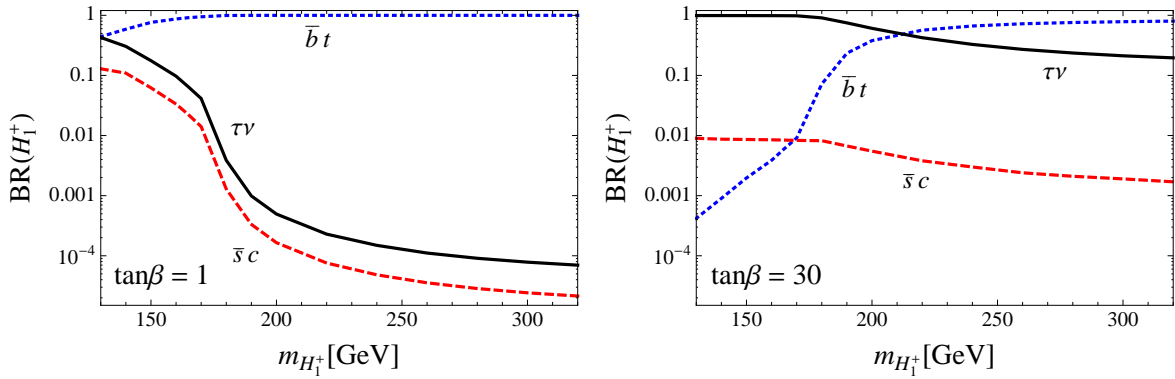


FIG. 4: Branching ratios for lighter charged Higgs decays as a function of $m_{H_1^\pm}$ with $\tan\beta = 1$ (left panel) and $\tan\beta = 30$ (right panel).

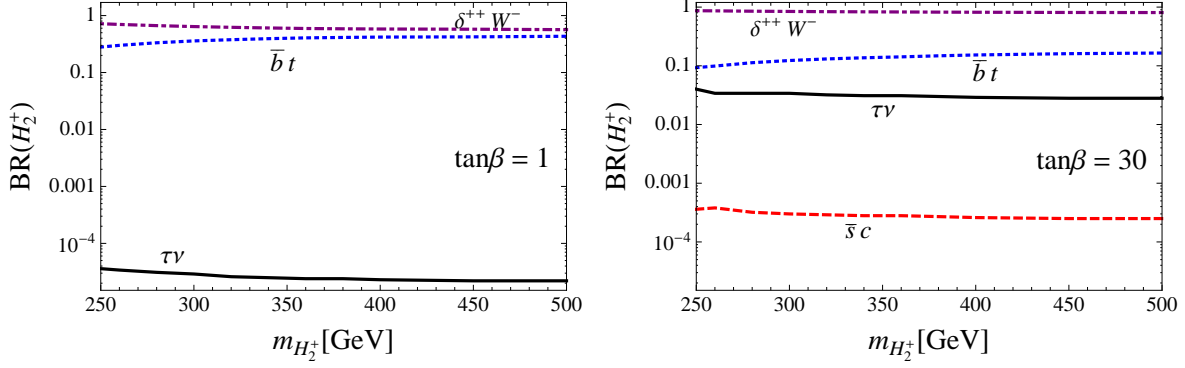


FIG. 5: The legend is the same as that in Fig. 4 but for H_2^+ .

IV. SIMULATION STUDIES

In this section, we discuss the possible signal/background events, the cuts for event selections and the significance for discovering the doubly charged Higgs. In order to generate the simulated events, we employ the event generator **MADGRAPH/MADEVENT 5** [35], where the necessary Feynman rules and relevant parameters of model are created by **FeynRules 2.0** [36]. We use **PYTHIA 6** [37] to deal with the fragmentation of hadronic effects, the initial-state radiation (ISR) and final-state radiation (FSR) effects, and the decays of SM particles e.g. W -boson, t -quark, etc. In event generation, we use the **NNPDF23L01** PDFs [38]. In addition, the generated events are also run through the **PGS 4** detector simulation [39]. In following analysis, we take collision energy at 13 TeV and the integrated luminosity is 40 fb^{-1} , which could be reached after 1 year running at 13 TeV [40, 41]. The results for 14 TeV should be similar.

A. Signals and backgrounds

The unique character of $\delta^{\pm\pm}$ is carrying two electric charges. For searching for the signals of $\delta^{\pm\pm}$, we require that the generated events at each collision have the same-sign charged lepton pairs $\ell^\pm \ell^\pm$ ($\ell = e, \mu$) in the final states. Unlike the cases in CTSM and Georgi-Machacek model [10, 30], where the same-sign dileptons are produced by $\delta^{\pm\pm}$ decays of leptonic channels directly or $W^\pm W^\pm$ channel, the production of $\ell^\pm \ell^\pm$ in our model is through more intermediate states. As mentioned before, the main decay channels of doubly charged

Higgs are

$$\delta^{\pm\pm} \rightarrow W^{\pm*} H_1^{\pm}, W^{\pm(*)} H_2^{\pm*}. \quad (16)$$

With the parameter settings in Eq. (14), the condition for the on-shell or off-shell W -boson depends on the mass of $\delta^{\pm\pm}$. Thus, one of the two same-sign leptons is emitted from this W -boson, e.g. $W^{(*)} \rightarrow \ell\nu_\ell$.

Furthermore, according to the interactions in Eq. (9) and Table I, we find that up to three-body decays, the dominant decay modes of H_1^{\pm} and $H_2^{\pm*}$ are

$$H_{1[2]}^{+(-)[*]} \rightarrow t^* \bar{b} (\bar{t}^* b) \rightarrow bW^+ \bar{b} (\bar{b}W^- b). \quad (17)$$

Therefore, the other lepton of the same-sign dilepton is from the on-shell W -boson which is emitted by top-quark. Since the same-sign dilepton from $\delta^{\pm\pm}$ are dictated by the processes shown in Eqs. (16) and (17), the kinematical distributions of the two leptons should be different from other Higgs triplet models. We will show the differences later. As to other particles produced during pp collision, we require them to convert into jets. Since there are more than four jets in the final states, the searching signals for $\delta^{\pm\pm}$ are set to be

$$\ell^\pm \ell^\pm + \text{four or more jets}. \quad (18)$$

The background events from the SM could mimic the signals of Eq. (18). For analyzing the backgrounds, we classify the possible processes as Drell-Yen (DY), EW, QCD, top and VV ($V = W$ or Z) backgrounds and write them as follows:

1. DY background : $pp \rightarrow l^+ l^- (+\text{ISR/FSR})$
2. EW background : $pp \rightarrow W^\pm W^\pm jj (\alpha^4)$
3. QCD background : $pp \rightarrow W^\pm W^\pm jj (\alpha^2 \alpha_s^2)$
4. top background : $pp \rightarrow W^\pm t \bar{t}, pp \rightarrow W^\pm t \bar{t} j$
5. VV ($V = W$ or Z) background : $pp \rightarrow W^\pm Z + nj, pp \rightarrow ZZ + nj$,

where the number of jets n for VV backgrounds is taken as $n \leq 2$ [10]. $W^\pm W^\pm + nj$ events in VV background have been included in EW and QCD background, therefore they should be excluded. Although DY processes in principle could contribute to the background, since the

second highest transverse momentum of the same-sign dilepton and transverse momenta of jets are small, their contributions indeed are negligible. We thus ignore the DY background in the simulation analysis.

B. Kinematical cuts

For enhancing the signals of $\delta^{\pm\pm}$ and reducing the possible backgrounds, we need to propose some strategies of kinematical cuts. For excluding the soft leptons and jets, when we generate the events by event generator, we set the preselection conditions for leptons and jets to be

$$\begin{aligned} p_T(\ell) &> 10 \text{ GeV}, \quad \eta(\ell) < 2.5, \\ p_T(j) &> 20 \text{ GeV}, \quad \eta(j) < 5.0, \end{aligned} \tag{19}$$

where p_T is the transverse momentum and $\eta = 1/2 \ln(\tan \theta/2)$ is pseudo-rapidity with θ being the scattering angle in the laboratory frame.

Since the signal processes have many b-jets in the final states, the number of b-tagging is a useful criterion to reject the backgrounds. In addition, differing from the CTSM and Georgi-Machacek model that both same-sign charged leptons have larger p_T , due to the small mass difference between $\delta^{\pm\pm}$ and H_1^\pm in the parameter settings, the charged lepton from the decay of $\delta^{\pm\pm} \rightarrow \ell^\pm \nu H_1^\pm$ has a lower p_T . For understanding clearly, we plot the histograms of events versus the transverse momentum of the second highest p_T lepton in Fig. 6, where we take $m_{\delta^{\pm\pm}} = (250, 500) \text{ GeV}$ and use the luminosity of 40 fb^{-1} . It is clear that the second highest p_T leptons of signal events prefer to locate at small p_T . Therefore, when we collect the events that are run through Pythia and PGS detector simulation, we further employ the new conditions for event selection as

$$N_{\text{b-jet}} \geq 1, \quad p_T(\ell_2) < 60 \text{ GeV}, \tag{20}$$

where $N_{\text{b-jet}}$ denotes the number of b-jet, ℓ_2 stands for the second highest p_T charged lepton and the upper limit of $p_T(\ell_2)$ is referred to the distributions in Fig. 6.

Besides $N_{\text{b-jet}}$ and $p_T(\ell_2)$, we also find that it is a useful method to reduce the backgrounds if we survey the invariant mass of the two same-sign leptons, denoted by $M_{\ell^\pm \ell^\pm}$. As discussed before, the same-sign leptons are generated through multiple intermediate states

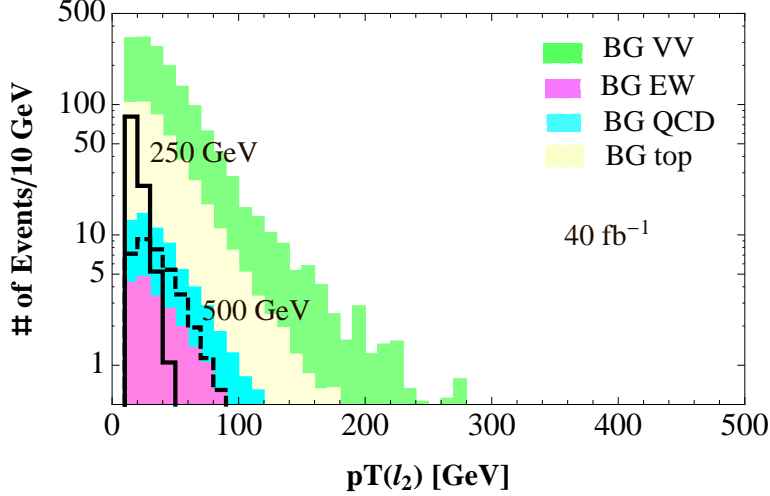


FIG. 6: Histograms of signal and background events versus $p_T(\ell_2)$, where the cuts of Eq. (19) and $m_{\delta^{\pm\pm}} = (250, 500)$ GeV are adopted. For normalizing the histograms, we use the luminosity of 40 fb^{-1} .

in $\delta^{\pm\pm}$ decays. It is expected that the major values of $M_{\ell^\pm\ell^\pm}$ are not large. We present the distributions of dilepton invariant mass for signals and backgrounds in Fig. 7, where the left panel results from the cuts of Eq. (19) and the right panel is arisen from the further cuts of Eq. (20). By the plots, we see that the signal events tend to locate at small region of the invariant mass. Consequently, we adopt the proper kinematical cut for $M_{\ell^\pm\ell^\pm}$ as

$$M_{\ell^\pm\ell^\pm} < \frac{m_{\delta^{\pm\pm}}}{4}. \quad (21)$$

Since the invariant mass distribution of signal does not have a peak at the mass of doubly charged Higgs, for extracting the mass value of $\delta^{\pm\pm}$, one needs to perform the fitting to the entire distribution with sufficient statistics.

C. Discovery potential

After establishing the criteria for event selection, we start to calculate the number of signals and each background events and investigate the resulting significance. In our calculations, the significance is defined by [42]

$$S = \sqrt{2[(n_s + n_b) \ln(1 + n_s/n_b) - n_s]}, \quad (22)$$

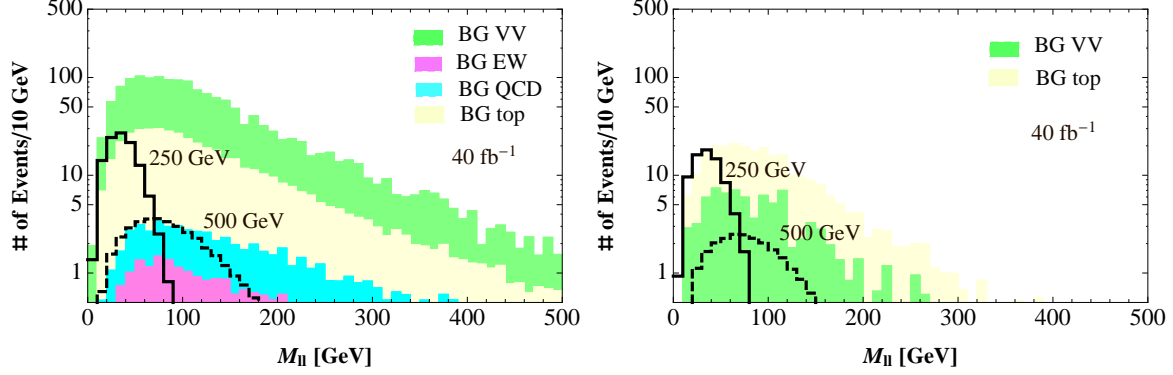


FIG. 7: Distributions of invariant mass of the same-sign dilepton with the basic cuts of Eq. (19) (left panel) and the additional cuts of Eq. (20) (right panel). For illustration, we take $m_{\delta^{\pm\pm}} = (250, 500)$ GeV and the luminosity of 40 fb^{-1} .

where n_s and n_b denote the number of signal and background events, respectively. For illustration, we take $m_{\delta^{\pm\pm}} = 200$ GeV and the integrated luminosity is set to be 40 fb^{-1} . Accordingly, after employing the kinematical cuts, the number of various events is shown in Table II. By the table, we see clearly that the condition with $N_{\text{b-jet}} \geq 1$ indeed can significantly eliminate the backgrounds, especially in the VV background. Furthermore, by using the cut of $M_{\ell^+\ell^+}$ proposed in Eq. (21), we find that the strongest competitor of signal is from the top background, in which the produced final states are similar to those from $\delta^{\pm\pm}$ decays.

cuts	signal	EW	QCD	$t\bar{t}$	VV	S
Basic cuts	81.2	22.3	44.2	398.	1095.	2.04
b-tagging	48.9	1.42	3.90	216.	92.6	2.69
$p_T(\ell_2^+) < 60 \text{ GeV}$	48.9	1.17	3.23	180.	72.8	2.96
$M_{\ell^+\ell^+} < 50 \text{ GeV}$	46.4	0.13	0.48	33.6	17.7	5.71

TABLE II: Number of signal and background events when the proposed kinematical cuts are applied, where we have used the luminosity of 40 fb^{-1} , $m_{\delta^{++}} = 200$ GeV and $\tan\beta = 1$. Both " $\ell^+\ell^++\text{jets}$ " and " $\ell^-\ell^-+\text{jets}$ " events are included.

In order to understand how the significance depends on the mass of $\delta^{\pm\pm}$ and what the value of luminosity is necessary to produce a 5σ observation of doubly charged Higgs, we plot

the related results in Fig. 8. The left (right) panel is the estimated significance (luminosity) as a function of $m_{\delta^{\pm\pm}}$. By the figure, one can find that the doubly charged Higgs boson with a mass lower than 330 GeV can be discovered at the LHC with an integrated luminosity of 40 fb^{-1} . Additionally, the doubly charged Higgs boson with a mass of 450 GeV can be discovered at the LHC with an integrated luminosity of 300 fb^{-1} which is a target luminosity of LHC at 13-14 TeV energy by the end of 2021 [40, 41].

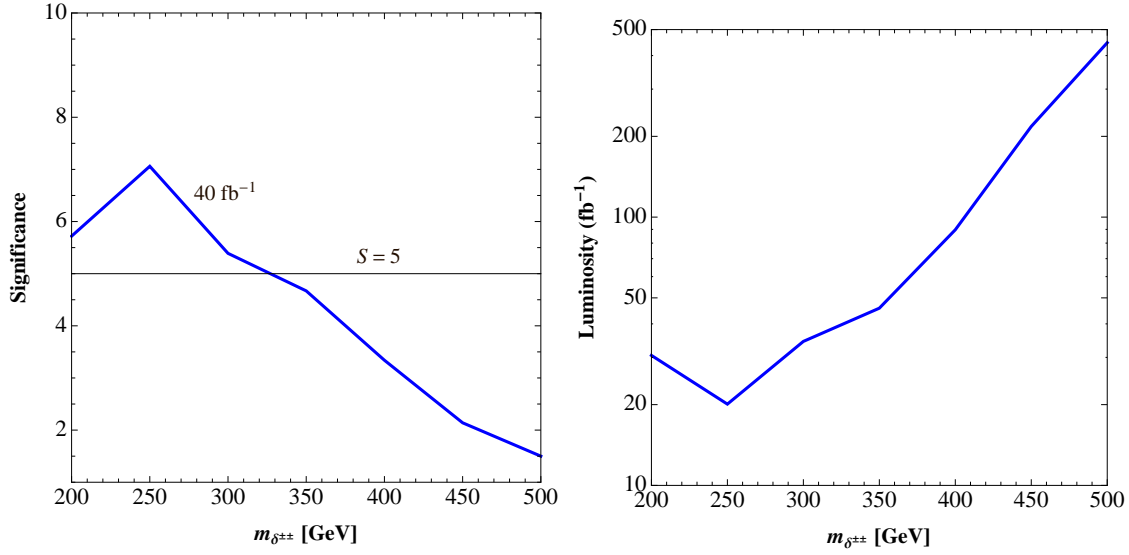


FIG. 8: Significance with 40 fb^{-1} (left) and luminosity for $S > 5$ (right) as a function of $m_{\delta^{\pm\pm}}$. The collision energy of 13 TeV is applied for both plots.

V. SUMMARY

We have studied the new properties of doubly charged Higgs and its discovery potential at the LHC in the THD extension of conventional type-II seesaw model. We find that the new dimension-3 interactions $\mu_j H_j^T i\tau_2 \Delta^\dagger H_k$ appearing in the scalar potential lead to a fantastic mixing effect between the singly charged Higgses of Higgs doublet and triplet. The mixing results completely different decay patterns in $\delta^{\pm\pm}$.

With small leptonic Yukawa couplings, $Y_{\ell\ell} \ll 1$, and $v_\Delta/v \ll 1$, due to the mixing effects, the doubly charged Higgs mostly decays into $W^{\pm*} H_1^\pm$ and $W^{\pm(*)} H_2^{\pm*}$, but not directly into $\ell\ell$ and WW modes which are usually discussed in the literature. That is, the search for doubly charged Higgs through either large $Y_{\ell\ell}$ or large v_Δ in experiments should be

reanalysed by the new decay channels. According to our analysis, it is found that in the considered model QCD processes are the predominant effects to produce the $\delta^{\pm\pm}$, read as $pp \rightarrow H_2^+ \bar{t}b(H_2^- t\bar{b}) \rightarrow \delta^{++}W^- \bar{t}b(\delta^{--}W^+ t\bar{b})$ and $\bar{b}(b)g \rightarrow H_2^+ \bar{t}(H_2^- t) \rightarrow \delta^{++}W^- \bar{t}(\delta^{--}W^+ t)$, while other Higgs triplet models are arisen from EW processes.

For searching for the signals of $\delta^{\pm\pm}$, besides the preselection cuts imposed in Eq. (19), in order to further reduce the background events and enhance the significance of signal, we also propose the kinematical cuts on the number of b-jets, $p_T(\ell_2)$ and the invariant mass of same-sign dilepton, defined in Eqs. (20) and (21). We find that with luminosity of 40 fb^{-1} and collision energy of 13 TeV, $\delta^{\pm\pm}$ with mass below 330 GeV could be observed at the 5σ level. Additionally, the observed mass of $\delta^{\pm\pm}$ could be up to 450 GeV when the luminosity approaches 300 fb^{-1} .

Acknowledgments

This work is supported by the Ministry of Science and Technology of R.O.C. under Grant #: MOST-103-2112-M-006-004-MY3 (CHC) and MOST-103-2811-M-006-030 (TN). We also thank the National Center for Theoretical Sciences (NCTS) for supporting the useful facilities.

-
- [1] G. Aad *et al.* [ATLAS Collaboration], Phys. Lett. B **716**, 1 (2012) [arXiv:1207.7214 [hep-ex]].
 - [2] S. Chatrchyan *et al.* [CMS Collaboration], Phys. Lett. B **716**, 30 (2012) [arXiv:1207.7235 [hep-ex]].
 - [3] P. Minkowski, Phys. Lett. B **67**, 421 (1977); T. Yanagida, Proceedings of the Workshop on Unified Theories and Baryon Number in the Universe, edited by A. Sawada and A. Sugamoto, (KEK Report No. 79-18, 1979); S. Glashow, in Quarks and Leptons, Cargese, 1979, edited by M. Lévy *et al.* (Plenum, New York, 1980); M. Gell-Mann, P. Ramond, and R. Slansky, Proceedings of the Supergravity Stony Brook Workshop, New York, edited by P. Van Nieuwenhuizen and D. Freedman (North-Holland, Amsterdam, 1979); R. N. Mohapatra and G. Senjanović, Phys. Rev. Lett. **44**, 912 (1980).
 - [4] M. Magg and C. Wetterich, Phys. Lett. B **94**, 61 (1980); G. Lazarides, Q. Shafi and C. Wetterich, Nucl. Phys. B **181**, 287 (1981); R. N. Mohapatra and G. Senjanovic, Phys. Rev. D **23**,

- 165 (1981); E. Ma and U. Sarkar, Phys. Rev. Lett. **80**, 5716 (1998) [hep-ph/9802445].
- [5] W. Konetschny and W. Kummer, Phys. Lett. B **70**, 433 (1977); J. Schechter and J. W. F. Valle, Phys. Rev. D **22**, 2227 (1980); T. P. Cheng and L. -F. Li, Phys. Rev. D **22**, 2860 (1980); S. M. Bilenky, J. Hosek and S. T. Petcov, Phys. Lett. B **94**, 495 (1980).
- [6] T. Han, B. Mukhopadhyaya, Z. Si and K. Wang, Phys. Rev. D **76**, 075013 (2007) [arXiv:0706.0441 [hep-ph]].
- [7] A. G. Akeroyd, M. Aoki and H. Sugiyama, Phys. Rev. D **77**, 075010 (2008) [arXiv:0712.4019 [hep-ph]]; A. G. Akeroyd and C. -W. Chiang, Phys. Rev. D **80**, 113010 (2009) [arXiv:0909.4419 [hep-ph]]; A. G. Akeroyd, C. -W. Chiang and N. Gaur, JHEP **1011**, 005 (2010) [arXiv:1009.2780 [hep-ph]];
- [8] F. del Aguila and J. A. Aguilar-Saavedra, Nucl. Phys. B **813**, 22 (2009) [arXiv:0808.2468 [hep-ph]];
- [9] M. Aoki, S. Kanemura and K. Yagyu, Phys. Rev. D **85**, 055007 (2012) [arXiv:1110.4625 [hep-ph]].
- [10] C. -W. Chiang, T. Nomura and K. Tsumura, Phys. Rev. D **85**, 095023 (2012) [arXiv:1202.2014 [hep-ph]].
- [11] H. Sugiyama, K. Tsumura and H. Yokoya, Phys. Lett. B **717**, 229 (2012) [arXiv:1207.0179 [hep-ph]];
- [12] S. Kanemura, K. Yagyu and H. Yokoya, Phys. Lett. B **726**, 316 (2013) [arXiv:1305.2383 [hep-ph]].
- [13] E. J. Chun and P. Sharma, Phys. Lett. B **728**, 256 (2014) [arXiv:1309.6888 [hep-ph]].
- [14] A. G. Akeroyd and M. Aoki, Phys. Rev. D **72**, 035011 (2005) [hep-ph/0506176]; A. G. Akeroyd and H. Sugiyama, Phys. Rev. D **84**, 035010 (2011) [arXiv:1105.2209 [hep-ph]].
- [15] A. Melfo, M. Nemevsek, F. Nesti, G. Senjanovic and Y. Zhang, Phys. Rev. D **85**, 055018 (2012) [arXiv:1108.4416 [hep-ph]].
- [16] E. J. Chun, K. Y. Lee and S. C. Park, Phys. Lett. B **566**, 142 (2003) [hep-ph/0304069];
- [17] P. Fileviez Perez, T. Han, G. -y. Huang, T. Li and K. Wang, Phys. Rev. D **78**, 015018 (2008) [arXiv:0805.3536 [hep-ph]];
- [18] A. Arhrib, R. Benbrik, M. Chabab, G. Moulhaka, M. C. Peyranere, L. Rahili and J. Ramadan, Phys. Rev. D **84**, 095005 (2011) [arXiv:1105.1925 [hep-ph]]; A. Arhrib, R. Benbrik, M. Chabab, G. Moulhaka and L. Rahili, JHEP **1204**, 136 (2012) [arXiv:1112.5453 [hep-ph]].

- [19] B. Dutta, R. Eusebi, Y. Gao, T. Ghosh and T. Kamon, Phys. Rev. D **90**, 055015 (2014) [arXiv:1404.0685 [hep-ph]].
- [20] P. S. Bhupal Dev, D. K. Ghosh, N. Okada and I. Saha, JHEP **1303**, 150 (2013) [Erratum-ibid. **1305**, 049 (2013)] [arXiv:1301.3453 [hep-ph]].
- [21] S. Chatrchyan *et al.* [CMS Collaboration], Eur. Phys. J. C **72**, 2189 (2012) [arXiv:1207.2666 [hep-ex]].
- [22] G. Aad *et al.* [ATLAS Collaboration], Eur. Phys. J. C **72**, 2244 (2012) [arXiv:1210.5070 [hep-ex]].
- [23] V. Khachatryan *et al.* [CMS Collaboration], arXiv:1410.6315 [hep-ex].
- [24] T. D. Lee, Phys. Rev. D **8**, 1226 (1973).
- [25] R. D. Peccei and H. R. Quinn, Phys. Rev. Lett. **38**, 1440 (1977).
- [26] P. M. Ferreira, R. Santos, H. E. Haber and J. P. Silva, Phys. Rev. D **87**, no. 5, 055009 (2013) [arXiv:1211.3131 [hep-ph]].
- [27] J. L. Diaz-Cruz, C. G. Honorato, J. A. Orduz-Ducura and M. A. Perez, arXiv:1403.7541 [hep-ph].
- [28] V. Barger, L. L. Everett, C. B. Jackson, A. D. Peterson and G. Shaughnessy, arXiv:1408.2525 [hep-ph].
- [29] C. H. Chen and T. Nomura, Phys. Rev. D **90**, 075008 (2014) [arXiv:1406.6814 [hep-ph]].
- [30] H. Georgi and M. Machacek, Nucl. Phys. B **262**, 463 (1985).
- [31] B. Pontecorvo, Sov. Phys. JETP **6**, 429 (1957) [Zh. Eksp. Teor. Fiz. **33**, 549 (1957)].
- [32] Z. Maki, M. Nakagawa and S. Sakata, Prog. Theor. Phys. **28**, 870 (1962).
- [33] A. Pukhov, [hep-ph/0412191].
- [34] P. M. Nadolsky, H. L. Lai, Q. H. Cao, J. Huston, J. Pumplin, D. Stump, W. K. Tung and C.-P. Yuan, Phys. Rev. D **78**, 013004 (2008) [arXiv:0802.0007 [hep-ph]].
- [35] J. Alwall, M. Herquet, F. Maltoni, O. Mattelaer and T. Stelzer, JHEP **1106**, 128 (2011) [arXiv:1106.0522 [hep-ph]].
- [36] A. Alloul, N. D. Christensen, C. Degrande, C. Duhr and B. Fuks, Comput. Phys. Commun. **185**, 2250 (2014) [arXiv:1310.1921 [hep-ph]].
- [37] T. Sjostrand, S. Mrenna, P. Z. Skands, JHEP **0605**, 026 (2006).
- [38] C. S. Deans [NNPDF Collaboration], arXiv:1304.2781 [hep-ph].
- [39] <http://www.physics.ucdavis.edu/conway/research/software/pgs/pgs4-general.htm>.

- [40] [CMS Collaboration], arXiv:1307.7135 [hep-ex].
- [41] [ATLAS Collaboration], arXiv:1307.7292 [hep-ex].
- [42] G. L. Bayatian *et al.* [CMS Collaboration], J. Phys. G **34**, 995 (2007).